Changes in the Interaction Mode of Bridging "C_2" Units According to Transition Metal Parameters: A Theoretical Approach

Paola Belanzoni, Nazzareno Re, Marzio Rosi, Antonio Sgamellotti,* and Carlo Floriani*

Dipartimento di Chimica, Università di Perugia, via Elce di Sotto 8, I-06123 Perugia, Italy, and Institut de Chimie Minérale et Analytique, BCH, Université de Lausanne, CH-1015 Lausanne, Switzerland

Received May 15, 1996[⊗]

A simple MO model allowing the prediction of the interaction mode of bridging "C_2" units in dinuclear complexes has been developed. The three possible limiting structures, namely M−C≡ C−M, M=C=C=M, and M≡C−C≡M, depend on the d^n configuration and the oxidation state of the transition metal and upon the nature of its ancillary ligands. These conclusions have been drawn on the basis of density functional calculations carried out on the model complexes $[\{(H_2O)_n(OH)_{3-n}M\}_2(\mu\text{-}C_2)]$ (M = Ti, V, Cr, Mn; n = 0, 1, 2) where the OH^- ligand mimics an OR^- ligand, a π-donor ligand which is widely used in organometallic chemistry. In addition, our calculations allowed the identification of two general classes of "C_2" bridged dinuclear transition metal complexes on the basis of the metal's parameters and position in the periodic table.

Introduction

In the context of metal−carbido chemistry, one naked C_n unit bonded to more than one transition metal has a particular relevance.[1−3] The $[C_2]$ unit bridging two metals may be considered the most simple synthetic building block in this respect[3−12] and is a fragment which has been known for a long time and which can be easily accessed both from acetylene and ethylene. Previous knowledge on the properties of $[M_2C_2]$ fragments has made easier the entry into its use for building up metal−carbides.

Even though all the three valence bond descriptions (Chart 1) have experimental support,[3] most of the synthesized complexes contain an acetylenic μ-C≡C bridge. A cumulenic *M*=*C*=*C*=*M* structure was found only in a few titanium and tantalum complexes, while a dimetalla-1,3-butadiyne structure *M*≡C−*C*≡M was observed only in the tungsten complex $[\{^t\text{BuO})_3W\}_2(\mu\text{-}C_2)]$.[3]

Chart 1

$$M - C \equiv C - M$$

$$M = C = C = M$$

$$M \equiv C - C \equiv M$$

Very few theoretical investigations have been performed on μ-C_2-bridged dinuclear complexes,[4,5,8] and these are mainly of semiempirical character.[4,8] Moreover, in spite of the interest drawn by this class of complexes, no clear criterion has been developed which enables one to forecast the valence bond structure on the basis of the characteristics of the two transition metal fragments, ML_m. In a critical survey of the literature on the dinuclear, transition metal, μ-C_2 bridged complexes,[3−12] two main classes of complexes can be identified, depending on the nature of the metal, its d configuration in the ML_m fragment, and the nature of the other ligands. A first class, hereafter called class I, is constituted by early transition metals (those of the titanium, vanadium, and chromium triads) in high oxidation states with mainly π-donor ligands like RO^- in a pseudotetrahedral coordination.[3−7] For this class of complexes, all three possible valence bond structures have been found depending on the metal's d configuration. A second class, hereafter called class II, is constituted by late transition metals (from the manganese triad to the right) in low oxidation states with mainly π-acceptor ligands (like carbonyl or phosphines) in a pseudo-octahedral coordination.[3,8−11] For this class of complexes, only the acetylenic μ-C≡C structure has been found, irrespective of the metal d configuration, which is d^7 in most of the cases. Depending on the oxidation state and the nature of the ligands, metal systems of the borderline chromium triad can be placed in both classes. Only very few complexes of early

* To whom correspondence should be addressed: A.G., Università di Perugia; C.F., BCH Université de Lausanne.

[⊗] Abstract published in *Advance ACS Abstracts,* August 15, 1996.

(1) Diederich, F.; Rubin, Y. *Angew. Chem., Int. Ed. Engl.* **1992**, *31*, 1101.
(2) Lang, H. *Angew. Chem., Int. Ed. Engl.* **1994**, *34*, 547.
(3) Beck, W.; Niemer, B.; Wieser, M. *Angew. Chem., Int. Ed. Engl.* **1993**, *32*, 923, and references therein.
(4) Neithamer, D. R.; LaPointe, R. E.; Wheeler, R. A.; Richeson, D. S.; Van Duyne, G. D.; Wolczanski, P. T. *J. Am. Chem. Soc.* **1989**, *111*, 9056.
(5) Caulton, K. G.; Cayton, R. H.; Chisholm, R. H.; Huffman, J. C.; Lobkovsky, E. B.; Xue, Z. *Organometallics* **1992**, *11*, 321.
(6) De Angelis, S.; Solari, E.; Floriani, C.; Chiesi-Villa, A.; Rizzoli, R. *Angew. Chem., Int. Ed. Engl.* **1995**, *34*, 1092.
(7) Binger, P.; Müller, P.; Philipps, P.; Gabor, B.; Mynott, R.; Herrmann, A. T.; Langhauser, F.; Krüger, C. *Chem. Ber.* **1992**, *125*, 2209.
(8) Heidrich, J.; Stelman, M.; Appel, M.; Beck, W.; Phillips, J. R.; Trogler, W. C. *Organometallics* **1990**, *9*, 1296.
(9) Davies, J. A.; El-Ghanam, M.; Pinkerton, A. A.; Smith, D. A. *J. Organomet. Chem.* **1991**, *409*, 367.
(10) Koutsantonis, G. A.; Selegue, J. P. *J. Am. Chem. Soc.* **1991**, *113*, 2316.
(11) Lemke, F. R.; Szalda, D. J.; Bullock, R. M. *J. Am. Chem. Soc.* **1991**, *113*, 8466.
(12) Chen, M. C.; Tsai, Y. J.; Lin, Y. C.; Tseng, T. W.; Lee, G. H.; Wang, Y. *Organometallics* **1991**, *10*, 378.

S0276-7333(96)00367-6 CCC: $12.00

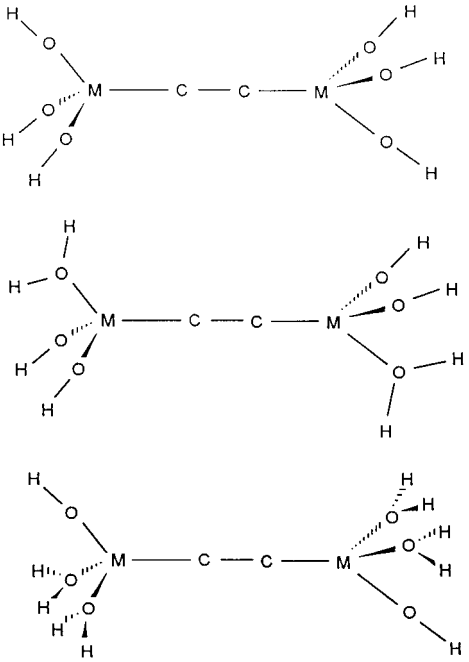

Figure 1. Geometrical structures of the model complexes.

transition metals in low oxidation states with π-acceptor ligands have been synthesized, and they behave as members of the second class.[12]

This paper addresses the theoretical study of class I of the complexes defined above. A special emphasis is put on the development of simple criteria which enable one to predict the structure of the relevant μ-acetylides on the basis of the metal fragment d configuration, the nature of the metal, its oxidation state, and the nature of the ligands. We have performed LCAO density functional calculations on a series of $[\{(H_2O)_n(OH)_{3-n}M\}_2(\mu\text{-}C_2)]$ (M = Ti, V, Cr, Mn; n = 0, 1, 2) complexes, see Figure 1, as models of the class of μ-acetylide-bridged complexes constituted by early to mid transition metals in high oxidation states, with π-donor ligands in a pseudotetrahedral coordination. The shift of M from Ti to Mn and of n from 0 to 2 permitted us to investigate both the effect of the change of the nature of the transition metal and of the variation of the fragment d configuration. We have found optimized structures consistent with all three possible valence bond structures, giving a rationale for their occurrence on the basis of the d configuration for the $[M(H_2O)_n(OH)_{3-n}]$ metal fragments and the relative energies of the corresponding d levels.

Computational Details

The calculations reported in this paper are based on the ADF (Amsterdam density functional) program package described elsewhere.[13−15] Its main characteristics are the use of a density fitting procedure to obtain accurate Coulomb and exchange potentials in each SCF cycle, the accurate and efficient numerical integration of the effective one-electron Hamiltonian matrix elements, and the possibility to freeze core orbitals. The molecular orbitals were expanded in an uncontracted double-ζ STO basis set for all atoms with the exception of the transition metal orbitals for which we used a double-ζ STO basis set for 3s and 3p and a triple-ζ STO basis set for 3d and 4s. As polarization functions, one 4p, one 3d and one 2p STO were used for transition metals, O and C, and H, respectively. The cores (Ti, V, Cr, Mn: 1s−2p; C, O, 1s) have been kept frozen.

The LDA exchange correlation potential and energy was used, together with the Vosko−Wilk−Nusair parametrization[16] for homogeneous electron gas correlation, including the Becke's nonlocal correction[3] to the local exchange expression and Perdew's nonlocal correction[18] to the local expression of correlation energy (NLDA). It has been demonstrated that excellent metal−metal and ligand−metal bond energies are obtained from this density functional based approach.[19] Molecular structures were optimized by the NLDA method, thanks to the successful implementation of analytical energy gradients, in D_{3d} symmetry for the $M_2C_2(OH)_6$ (M = Ti, V,Cr, Mn) and in C_{2h} symmetry for $M_2C_2(OH)_4(H_2O)_2$ and $M_2C_2(OH)_2(H_2O)_2$ (M = Ti, Cr) systems. Multiplet energies and singlet−triplet splittings have been computed according to the method by Ziegler et al.[20]

Table 1. Geometrical Parameters of Titanium, Vanadium, Chromium, and Manganese Complexes in D_{3d} Symmetry, with Bond Lengths in Å and Bond Angles in deg

param	$Ti_2C_2(OH)_6$	$V_2C_2(OH)_6$	$Cr_2C_2(OH)_6$	$Mn_2C_2(OH)_6$
C−C	1.241	1.268	1.314	1.276
M−C	2.047	1.882	1.748	1.781
M−O	1.817	1.806	1.795	1.772
O−H	0.977	0.984	0.993	0.993
∠OMC	107.0	105.7	105.3	104.2
∠MOH	141.0	120.2	109.2	108.2
∠OMO	111.9	113.0	113.3	114.2

Table 2. Geometrical Parameters of Titanium Complexes, with Bond Lengths in Å and Bond Angles in deg[a]

param	$Ti_2C_2(OH)_6$ (D_{3d})	$Ti_2C_2(OH)_4(H_2O)_2$ (C_{2h})	$Ti_2C_2(OH)_2(H_2O)_4$ (C_{2h})
C−C	1.241	1.277	1.362
Ti−C	2.047	1.946	1.843
Ti−O	1.817	1.871	1.866
Ti−O′		2.249	2.200
O−H	0.977	0.978	0.982
O′−H′		0.984	0.984
∠OTiC	107.0	111.3	109.2
∠O′TiC		103.0	85.8
∠TiOH	141.0	129.4	119.5
∠OTiO	111.9	131.2	
∠O′TiO′			125.4
∠TiCC		174.0	173.1
∠H′O′H′		107.4	107.0

[a] The prime sign refers to the H_2O ligand.

Results

For all of these complexes the ground state is a singlet $^1A_{1g}$, with the exception of $[\{(OH)_3V\}_2(\mu\text{-}C_2)]$ and $[\{(OH)_3Mn\}_2(\mu\text{-}C_2)]$ for which a triplet $^3A_{2g}$ ground state has been found. The optimized geometrical parameters of all the $[\{(H_2O)_n(OH)_{3-n}M\}_2(\mu\text{-}C_2)]$ species considered are shown in Tables 1−3. Table 1 illustrates the optimized

(13) (a) Baerends, E. J.; Ellis, D. E.; Ros, P. *Chem. Phys.* **1973** *2*, 42. (b) Baerends, E. J.; Ros, P. *Chem. Phys.* **1973**, *2*, 51. (c) Baerends, E. J.; Ros, P. *Chem. Phys.* **1975**, *8*, 41. (d) Baerends, E. J.; Ros, P. *Int. J. Quantum Chem.* **1978**, *S12*, 169.

(14) (a) Boerrigter, P. M.; te Velde, G.; Baerends, E. J. *Int. J. Quantum Chem.* **1988**, *33*, 87. (b) Te Velde, G.; Baerends, E. J. *J. Comput. Phys.* **1992**, *99*, 84.

(15) Ziegler, T.; Tschinke, V.; Baerends, E. J.; Snijders, J. G.; Ravenek, W. *J. Phys. Chem.* **1989**, *93*, 3050.

(16) Vosko, S. H.; Wilk, L.; Nusair, M. *Can. J. Phys.* **1980**, *58*, 1200.

(17) Becke, A. D. *Phys. Rev.* **1988**, *A38*, 2398.

(18) Perdew, J. P. *Phys. Rev.* **1986**, *B33*, 8822.

(19) Versluis, L.; Ziegler, T. *J. Chem. Phys.* **1988**, *88*, 322.

(20) Ziegler, T.; Rauk, A.; Baerends, E. J. *Theoret. Chim. Acta* **1977**, *43*, 261.

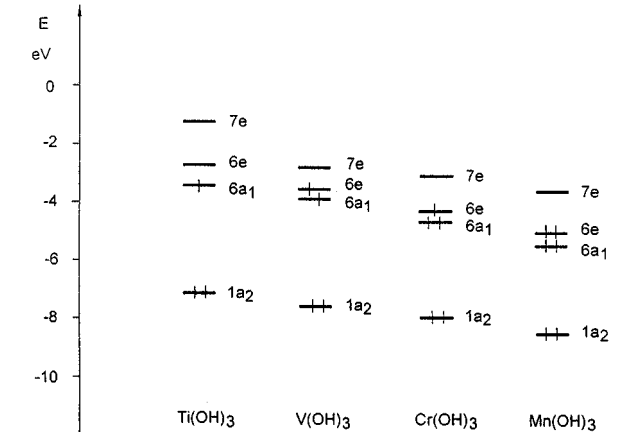

Figure 2. Energies of the main frontier orbitals for the $[M(OH)_3]$ metal fragments.

Table 3. Geometrical Parameters of Chromium Complexes, with Bond Lengths in Å and Bond Angles in deg[a]

param	$Cr_2C_2(OH)_6$ (D_{3d})	$Cr_2C_2(OH)_4(H_2O)_2$ (C_{2h})	$Cr_2C_2(OH)_2(H_2O)_4$ (C_{2h})
C−C	1.314	1.332	1.346
Cr−C	1.748	1.722	1.775
Cr−O	1.795	1.802	1.808
Cr−O′		2.394	2.380
O−H	0.993	0.984	0.978
O′−H′		0.986	0.982
∠OCrC	105.3	105.4	130.2
∠O′CrC		144.8	120.4
∠CrOH	109.2	113.8	171.2
∠OCrO	113.3	120.4	
∠O′CrO′			90.1
∠CrCC		179.2	173.2
∠H′O′H′		104.9	106.8

[a] The prime sign refers to the H_2O ligand.

geometries in the $[\{(OH)_3M\}_2(\mu\text{-}C_2)]$ (M = Ti, V, Cr, Mn) complexes of D_{3d} symmetry, while Tables 2 and 3 illustrate the optimized geometries of the $[\{(H_2O)_n(OH)_{3-n}Ti\}_2(\mu\text{-}C_2)]$ and $[\{(H_2O)_n(OH)_{3-n}Cr\}_2(\mu\text{-}C_2)]$, ($n$ = 0, 1, 2) complexes of D_{3d} or C_{2h} symmetry.

To discuss the results, it is convenient to consider a fragment approach in which two $[M(H_2O)_n(OH)_{3-n}]$ fragments interact with a C_2 species along a common MCCM axis. However, such an approach leads to an electron count for the metal in the $[M(H_2O)_n(OH)_{3-n}]$ fragments slightly different from the electron count which would be considered for the metal in the whole dinuclear complex on the basis of formal oxidation state assignments.

The $[M(H_2O)_n(OH)_{3-n}]$ fragments have been considered in a pseudotrigonal pyramidal structure, of C_{3v} symmetry if n = 0 or C_s if n ≠ 0, with the same geometries obtained in the optimization of the corresponding dinuclear complexes, and their valence MOs are reported in Figures 2 and 3. The valence orbitals of the $[M(H_2O)_n(OH)_{3-n}]$ fragment can be divided into two groups. The first group of orbitals consists of low-lying occupied MOs which describe essentially the M−O and O−H bonds and nonbonding p-type orbitals of oxygen. The second group consists of the five orbitals which are higher in energy, unoccupied or singly occupied depending on the d configuration, and are essentially of metal d character. In more detail, for the fragments of C_{3v} symmetry the d orbitals are made up of a $6a_1$ which is essentially an $s-d_{z^2}$ hybrid, a doubly degenerate 6e, whose components are mainly metal d_{xz} and d_{yz} orbitals of d_π character, and a doubly degenerate 7e, whose components are mainly $d_{x^2-y^2}$ and d_{xy} orbitals of d_δ character. However, in the C_{3v} symmetry, the d_π and d_δ components can mix and, actually, the 6e and 7e orbitals present small d_δ and d_π components, respectively. This picture is in agreement with the usual qualitative description of the C_{3v} ML_3 fragment based on extended Hückel theory.[21] For the fragments belonging to the C_s point group, the d orbitals are similar,

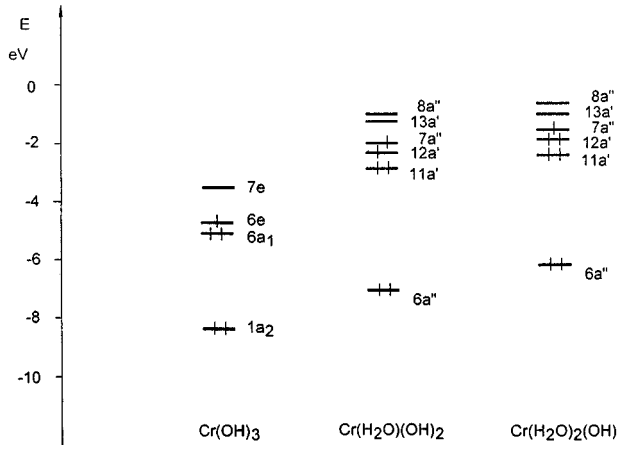

Figure 3. Energies of the main frontier orbitals for the $[Cr(OH)_{3-n}(H_2O)_n]$ metal fragments.

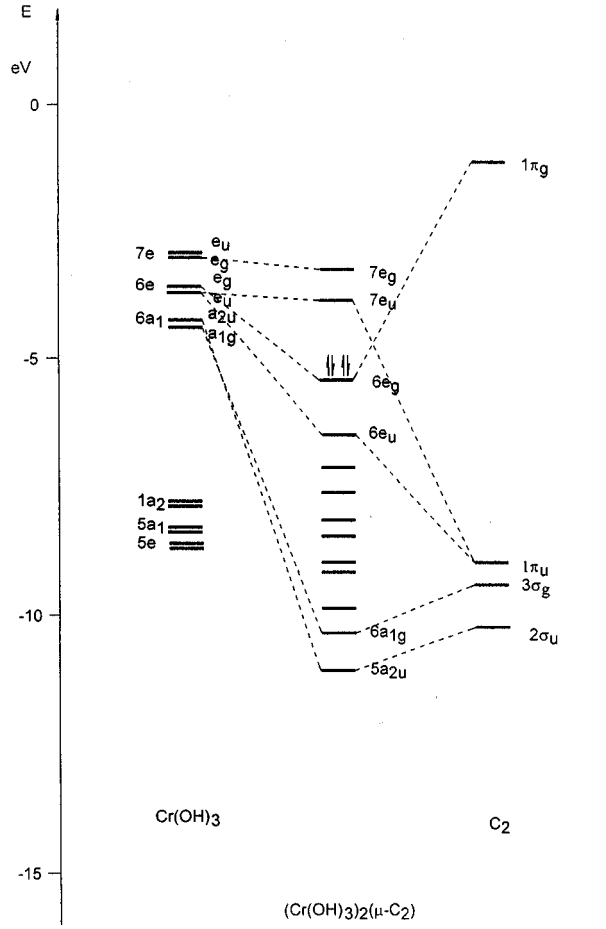

Figure 4. Molecular orbital diagram for the $[\{(OH)_3Cr\}_2(\mu\text{-}C_2)]$ complex depicting the interactions between the frontier orbitals of $[Cr(OH)_3]$ and C_2.

(21) Albright, T. A.; Burdett, J. K.; Whangbo, M. H. *Orbital Interactions in Chemistry*; John Wiley & Sons: NewYork, 1985.

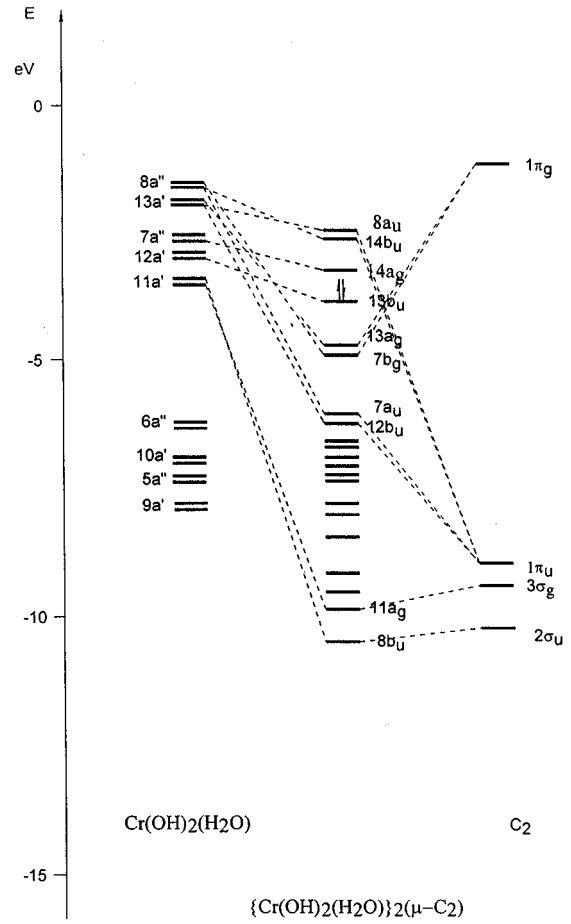

Figure 5. Molecular orbital diagram for the [{$(OH)_2(H_2O)$-Cr}$_2(\mu$-$C_2)$] complex depicting the interactions between the frontier orbitals of [$Cr(OH)_2(H_2O)$] and C_2.

although the situation is complicated by the lower symmetry which removes the degeneracy of the e orbitals and mixes the d_σ, d_π, and d_δ components. They are now made up of the 11a′, a metal s−d_{z^2} hybrid, the 12a′ and 7a″, of mainly d_δ character, and the 13a′ and 8a″, of mainly d_π character.

The C_2 molecule has been considered in the $^3\Sigma_u$ state, $(1\pi_u)^4(3\sigma_g)^1(2\sigma_u)^1$ configuration, corresponding to the valence state, with a bond distance equal to that found in the corresponding [{$(H_2O)_n(OH)_{3-n}M\}_2(\mu$-$C_2)$] complex. Its main valence orbitals are depicted on the right in Figures 4 and 5. The singly occupied $3\sigma_g$ and $2\sigma_u$ correspond to the in-phase and out-of-phase combinations of the carbon sp hybrids and are of the right symmetry to interact with the metal d_σ orbitals. The HOMO $1\pi_u$ corresponds to the two orthogonal π orbitals while the LUMO $1\pi_g$ corresponds to the two π* orbitals.

Figures 4 and 5 show the MOs for the two [$M(H_2O)_n(OH)_{3-n}$] fragments interacting with the MOs of the bridging C_2 ligand to reproduce the energy levels of the [{$(H_2O)_n(OH)_{3-n}M\}_2(\mu$-$C_2)$] complex most relevant to metal-carbon bonding for two representive cases of D_{3d} and C_{2h} symmetry: M = Cr with n = 0 or 1. In these figures we report the energy levels for the two [$M(H_2O)_n(OH)_{3-n}$] fragments at the same distance observed in the whole complex (ca. 5 Å). Due to extremely small interactions between the two fragments, these levels consist of almost degenerate symmetric and antisymmetric combinations of the levels for the single fragment. These combinations can also be classified in terms of the irreducible representations of the symmetry group of the whole complex, as reported in Figure 4 for the most relevant levels. On the right of Figures 4 and 5, we also report the main valence orbitals of the C_2 molecule as described above. In all of these complexes, the bonding orbitals between metal atoms and the bridging C_2 molecule can be divided into three groups:

Three low-lying orbitals describe the σ C−C and M−C bonds, which constitute the M−C−C−M σ skeleton. They are formed by the in-phase and out-of-phase d_σ orbitals of the [$M(H_2O)_n(OH)_{3-n}$] fragments interacting with the $3\sigma_g$ and $2\sigma_u$ orbitals of C_2 and by the mainly pure $2\sigma_g$ orbital of C_2.

Two low-lying orbitals essentially describe the two π bonds of C_2 and are formed mainly by the $1\pi_u$ orbitals of C_2 slightly interacting with the out-of-phase combination of the d_π orbitals of the metal fragments.

A group of higher-lying orbitals, occupied or empty depending on the system considered, constitute essentially the $\pi-\delta$ system.

The first two groups are close in energy to the orbitals describing the M−O and O−H bonds and the lone pairs of oxygens. The orbitals of the latter group describe the metal−carbon π bonds and are by far the most important: they will be discussed in more detail in the next section. In the [{$(OH)_3M\}_2(\mu$-$C_2)$] complexes of D_{3d} symmetry, the most important frontier orbitals which describe the metal−carbon $\pi-\delta$ system are the $6e_u$, $6e_g$, $7e_u$, and $7e_g$ ones, whose composition is illustrated in Table 4. In particular, we see that $6e_u$ essentially describes the two π bonds of C_2 and $6e_g$ and $7e_u$ essentially describe the $d_\pi-\pi^*$ (C_2) and $d_\pi-\pi$ (C_2) interactions, respectively, while $7e_g$ describes the metal d_δ orbitals. In the [{$(H_2O)_n(OH)_{3-n}M\}_2(\mu$-$C_2)$], $n \neq 0$, complexes of C_{2h} symmetry the main frontier orbitals are $7a_u$, $12b_u$, $7b_g$, $13a_g$, $8a_u$, $14b_u$, $13b_u$, and $14a_g$, illustrated in Table 5. Figure 5, which is representive of all other C_{2h} complexes, shows that these orbitals are close in energy by pairs, while Table 5 illustrates that

Table 4. Composition of the Main Frontier Orbitals for Complexes of D_{3d} Symmetry

orbital	composn
$6e_u$	$\pi_y(C_2) + (d_{yz} - d'_{yz})$
	$\pi_x(C_2) + (d_{xz} - d'_{xz})$
$6e_g$	$(d_{yz} + d'_{yz}) + \pi^*_y(C_2)$
	$(d_{xz} + d'_{xz}) + \pi^*_x(C_2)$
$7e_u$	$(d_{yz} - d'_{yz}) - \pi_y(C_2)$
	$(d_{xz} - d'_{xz}) - \pi_x(C_2)$
$7e_g$	$(d_{x^2-y^2} + d'_{x^2-y^2})$
	$(d_{xy} + d'_{xy})$

Table 5. Composition of the Main Frontier Orbitals for Complexes of C_{2h} Symmetry

orbital	composn
$7a_u$	$\pi_y(C_2) + (d_{yz} - d'_{yz})$
$12b_u$	$\pi_x(C_2) + (d_{xz} - d'_{xz})$
$7b_g$	$(d_{yz} + d'_{yz}) + \pi^*_y(C_2)$
$13a_g$	$(d_{xz} + d'_{xz}) + \pi^*_x(C_2)$
$8a_u$	$(d_{yz} - d'_{yz}) - \pi_y(C_2)$
$14b_u$	$(d_{xz} - d'_{xz}) - \pi_x(C_2)$
$13b_u$	$(d_{xy} - d'_{xy})$
$14a_g$	$(d_{xy} + d'_{xy})$

the nature of these four pairs corresponds with that of the four orbitals for the D_{3d} complexes described above.

Discussion

All the results presented in the previous section can be interpreted with a simple molecular orbital scheme for four-center M−C−C−M π and δ interactions, analogous to that proposed to explain bonding in dinitrogen-bridged transition metal dimers[22] and already employed to interpret the results of *ab initio* calculations on these complexes.[23−25] This parallel with the chemistry of linear bridged dinitrogen complexes has already been proposed[5] but not yet fully exploited. In such a model, we assume the following energy order of the bridging orbitals classified on the basis of their symmetry with respect to the M−C−C−M axis (assumed to be the z axis): $\sigma \ll \pi \leq \delta \leq \delta^* \leq \pi^* \ll \sigma^*$. In other words, we assume that the lowest metal d_{z^2} orbitals strongly interact with the sp hybrid of each carbon forming two low-lying MOs describing M−C σ bonds, while two other carbon sp hybrids form the C−C σ bond MO at an even lower energy. The uppermost frontier orbitals pertinent to the bonding in the dicarbide bridge are therefore those originating from the interactions of the carbon π and the metal d_π orbitals and from the d_δ orbitals. The π-system is constituted by the four-center molecular orbitals reported in Chart 2.

There are actually two sets of these four-center molecular orbitals which are obtained by linear combinations of Md_{xz}, Cp_x or Md_{yz}, Cp_y orbitals. As an overall result, we have four doubly degenerate energy levels

Chart 2

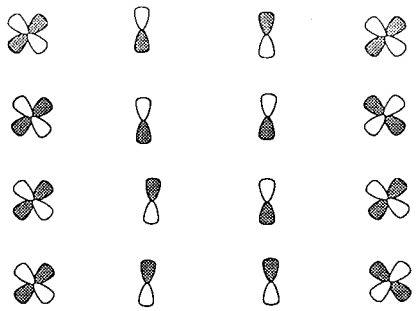

whose energies increase with increasing nodal planes and which are designated as $1\pi-4\pi$. In this context, it is more useful to consider the four-center molecular orbitals as being built by the proper combinations of the π and π^* orbitals of the C_2 moiety with the metal d_π orbitals. Two of them, 1π and 3π, will therefore have a C_2 π-bonding character, while the other two, 2π and 4π, have a C_2 π^*-antibonding character. The scheme is completed by the orbitals of δ symmetry built by the bonding and antibonding combinations of the d_{xy} and, eventually, also the $d_{x^2-y^2}$ orbitals, depending on the geometry of the L_mM fragment. These orbitals do not interact with any C_2 orbital and give no contribution to the bonding; they should lay between 2π and 4π and will be designated as $1\delta-4\delta$. The nature of the metals and of the ligands and the coordination geometry in the metal fragments determine the energy of the metal d orbitals and, therefore, both the metal character of the $1\pi-4\pi$ orbitals and the relative position of the $1\delta-4\delta$ levels. If the σ $M-C-C-M$ skeleton is regarded as mainly constant, the variation in the M−C and C−C bond character can be attributed to changes in the nature and in the occupancy of the frontier orbitals. For complexes of class I, the unoccupied or singly occupied metal d orbitals, destabilized by their interactions with the π-donor ligands, are usually much higher in energy than the C_2 π orbitals and the 1π level corresponds essentially to the $1\pi_u$ MO of the C_2 molecule, of C−C π bonding character. Moreover, the $2\pi-4\pi$ orbitals possess higher metal character and the pure metal $1\delta-4\delta$ orbitals lie between them.

When the occupancy of these levels is taken into account, it is convenient, to be consistent with the previous calculations, to perform the electron count considering a neutral C_2 molecule bracketed by the two metal ML_m fragments. Therefore, the d^n configuration attributed to the ML_n fragment is at least one unit higher than that attributable to the metal in the whole complex on the basis of the formal oxidation state assignment. If each L_mM fragment has a d^n configuration, a total of $2(n-1)+4$ electrons are left to occupy these π and δ frontier orbitals, four coming from the C_2 unit and $n-1$ from each metal fragment.

The four electrons from the C_2 π orbitals invariably fill the 1π level. This MO essentially describes two π bonds between the carbon atoms, although, due to its partial metal character, a slighty lower C−C bond order would be associated with it. For metal fragments L_mM with a d^1 configuration, this is the only filled π-type orbital, and an acetylenic $M-C\equiv C-M$ structure is expected. The progressive occupation of the higher 2π level, of C−C antibonding and M−C bonding character, leads to a relevant weakening of the C−C bond and to

(22) Chatt, J.; Fay, R. C.; Richards, R. L. *J. Chem. Soc. A* **1971**, 2399. Treitel, J. M.; Flood, M. T.; March, R. E.; Gray, H. B. *J. Am. Chem. Soc.* **1969**, *91*, 6512. Sellmann, D. *Angew. Chem., Int. Ed. Engl.* **1974**, *13*, 639.

(23) Re, N.; Rosi, M.; Sgamellotti, A.; Floriani, C.; Solari, E. *Inorg. Chem.* **1994**, *33*, 4390.

(24) Re, N.; Rosi, M.; Sgamellotti, A.; Floriani, C. *Inorg. Chem.* **1995**, *34*, 3410.

(25) Powell, C. B.; Hall, M. B. *Inorg. Chem.* **1984**, *23*, 4619.

a strengthening of the M−C bonding. This level will be filled for a d^3 configuration of the metal fragment formally giving a M≡C−C≡M valence bond structure. For example, such a situation has been observed in the tungsten complex $[\{(^tBuO)_3W\}_2(\mu\text{-}C_2)]$.[5] For a d^2 configuration of the ML_m fragment, the 2π level will be occupied by two electrons giving a cumulenic M=C=C=M structure. This is observed, for instance, in the tantalum and titanium complexes $[\{^tBu_3SiO)_3Ta\}_2(\mu\text{-}C_2)]$,[4] $[\{Cp_2(PMe_3)Ti\}_2(\mu\text{-}C_2)]$,[7] and $[\{Et_8N_4)_3Ti\}_2(\mu\text{-}C_2)(\mu Li)_2]^{2-}$ (Et_8N_4 = *meso*-octaethylporphirinogen).[6] Moreover, the double degeneracy of this level allowed us to forecast—provided that the M−C−C−M unit remains perfectly linear with an overall molecular symmetry high enough—a triplet ground state.

The filling of the $1\delta-4\delta$ levels for fragments with more than 3 d electrons does not affect the C−C and M−C bonds. On the other hand, the occupation of the 3π level, one of C−C bonding and M−C antibonding character, will result in an increase of the C−C and a decrease of the M−C bond distances. The complete filling of this level would lead to an acetylenic M−C≡C−M structure, although this can never be observed for class I complexes where the metal fragments have few d electrons.

Although not directly considered in this work, a few preliminary calculations on complexes belonging to class II permit some general considerations of these systems. Indeed, for complexes belonging to class II, the doubly occupied metal d_π orbitals, stabilized by interactions with π-acceptor ligands, are usually lower in energy than the C_2 π orbitals. In this case, the 1π and 2π orbitals are mainly of metal character while the 3π level has a high C_2 π contribution. Moreover, for a pseudo-octahedral eclipsed coordination of the metal fragment usually found in this class, the $d_{x^2-y^2}$ levels are destabilized by interactions with equatorial ligands, leaving only two δ levels at energies between that of the 2π and 3π orbitals. We would then expect a complete filling of the $1\delta-2\delta$ and the 3π orbitals, with a singlet ground state and a formal acetylenic structure, for a d^7 configuration of the metal fragment L_mM. In the most of the μ-C_2-bridged dinuclear complexes belonging to class II, the metal fragment configuration is invariably d^7 and the structure is always acetylenic. These systems will be the subject of a forthcoming paper.

The difference between the molecular orbital diagrams for these two classes of complexes is better illustrated in Figures 6 and 7, where we show the interaction diagrams between the C_2 π and π^* MOs and the symmetric and antisymmetric combinations of the metal fragments d orbitals. The VB structures for these complexes, forecast on the basis of the metal d configuration of the ML_m fragments, is summarized in Chart 3.

Geometries. The calculated C−C and M−C bond distances in the $[\{(OH)_3M\}_2(\mu\text{-}C_2)]$ (M = Ti, V, Cr, Mn) and $[\{(H_2O)_n(OH)_{3-n}M\}_2(\mu\text{-}C_2)]$ (M = Ti, Cr; n = 0, 1, 2) series are in good agreement with the model previously described. Table 1 illustrates that going from Ti to Cr in the $[\{(OH)_3M\}_2(\mu\text{-}C_2)]$ series of D_{3d} symmetry, *i.e.* going from a d^1 to a d^3 configuration of the $[M(OH)_3]$ fragment, there is a lengthening of the C−C bond and a shortening of the M−C bond. On the other hand, when we pass to the Mn species, for which the fragment

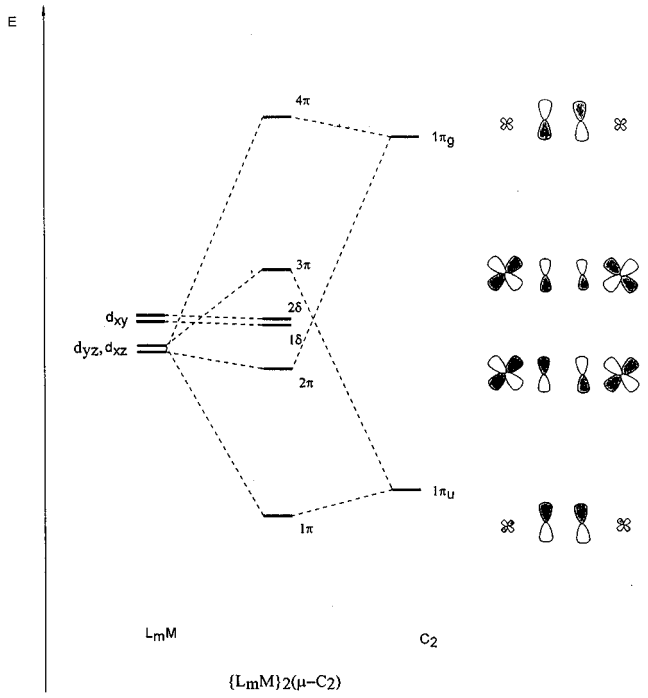

Figure 6. Schematic molecular orbital diagram for L_m-MC_2ML_m complexes of class I depicting the main interactions between the frontier orbitals of $[ML_m]$ and C_2.

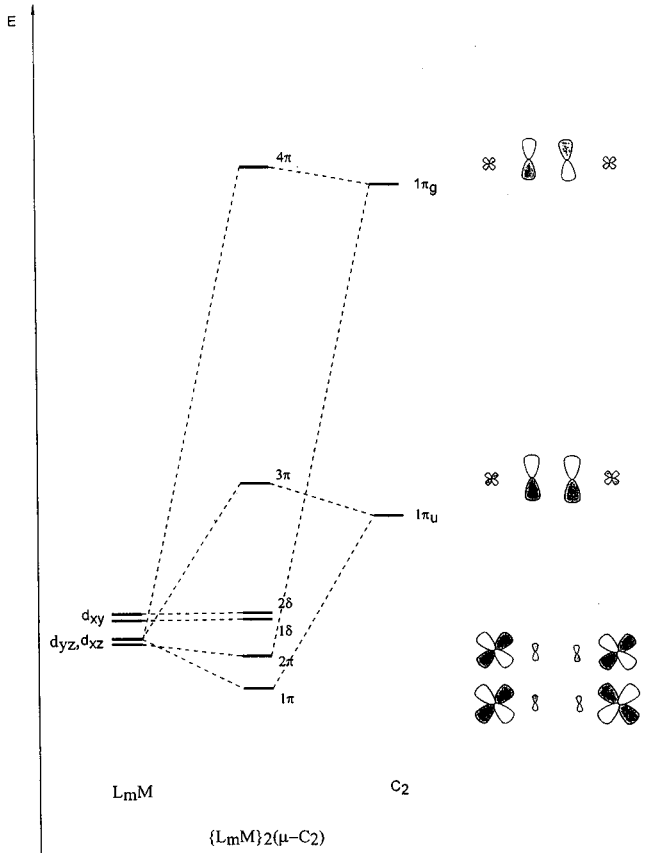

Figure 7. Schematic molecular orbital diagram for L_m-MC_2ML_m complexes of class II depicting the main interactions between the frontier orbitals of $[ML_m]$ and C_2.

$[M(OH)_3]$ has a d^4 configuration, there is a shortening of the C−C bond and a small lengthening of the M−C bond with respect to chromium. In particular, we see that the C−C bond lengths in the Ti, V, and Cr species are 1.241, 1.268, and 1.314 Å, respectively, which are

Chart 3

Class	Fragment *d* configuration	Bond character
Class I	d^1	$M-C\equiv C-M$
	d^2	$M=C=C=M$
	d^3	$M\equiv C-C\equiv M$
Class II	d^7,..	$M-C\equiv C-M$

close to the values reported for the corresponding hydrocarbons with triple, double, and single C−C bonds. We must take into account that the right comparison should be made with single, double, and triple bonds between sp-hybridized carbons. So, while for a MC≡CM triple bond the most pertinent comparison can be made with ethyne (1.212 Å), for a MC═CM double bond such a comparison is provided by the central C−C distance in cumulene (1.284 Å) and for a MC−CM single bond by the central C−C distance in 1,3-butadiyne (1.384 Å). More difficult is the assignment of bond orders of the M−C bonds on the basis of the optimized M−C bond lengths because of the absence of data for multiple Ti−C and V−C bonds. However, we can say that Cr−C bond distance of 1.748 Å is in the range of distances expected for Cr−C triple bonds, 1.65−1.79 Å, while the Ti−C distance of 2.047 Å is similar to other observed single Ti−C bonds. The V−C bond distance of 1.882 Å has an intermediate value which can be resonably assigned to a double bond. All these results match very well with the qualitative model described above, with the d^1, d^2, and d^3 configurations of the $M(OH)_3$ metal fragments leading, respectively, to M−C≡C−M, M═C═C═M, and M≡C−C≡M VB descriptions. The behavior of the Mn complex is less easy to interpret. Indeed, in this case, the $Mn(OH)_3$ fragments have a d^4 configuration and the two electrons in excess with respect to the chromium complex should occupy a δ orbital without affecting the C−C and M−C bonds. However, a relevant shortening is observed in the C−C bond distance which shows a value close to that of a C−C double bond, 1.276 Å, while a corresponding lengthening is observed for the M−C bond distance. As we will see below, this is due to the occupation of a 3π orbital of C_2 π^* character by the two excess electrons.

The trend of the optimized geometrical parameters calculated for the $[\{(H_2O)_n-(OH)_{3-n}Ti\}_2(\mu\text{-}C_2)]$ and $[\{(H_2O)_n(OH)_{3-n}Cr\}_2(\mu\text{-}C_2)]$ (n = 0, 1, 2) series (see Tables 2 and 3) can also be immediately explained in terms of the above qualitative model. Table 2 illustrates that going from n = 0 to 2 in the $[\{(H_2O)_n(OH)_{3-n}Ti\}_2(\mu\text{-}C_2)]$ series (*i.e.* going from a d^1 to a d^3 configuration of the $[Ti(H_2O)_n(OH)_{3-n}]$ fragment) there is a lengthening of the C−C bond and a shortening of the M−C bond, exactly as observed in the $[\{(OH)_3M\}_2(\mu\text{-}C_2)]$ (M = Ti, V, Cr) series discussed above. On the other hand, Table 3 illustrates that going from n = 0 to 2 in the $[\{(H_2O)_n(OH)_{3-n}Cr\}_2(\mu\text{-}C_2)]$ series (*i.e.* going from a d^3 to a d^5 configuration of the $[Cr(H_2O)_n(OH)_{3-n}]$ fragment) there is only a slight variation of the C−C and M−C bonds, all three complexes being consistent with M≡C−C≡M VB descriptions. This behavior is different from that observed for the $[\{(OH)_3Mn\}_2(\mu\text{-}C_2)]$ complex with a d^4 fragment configuration and, as we will see below, is due to the occupation of the d electrons of the $1\delta-2\delta$ orbitals before the 3π orbital.

Bonding Considerations. Coming back to the results of our calculations, we can see that the calculated frontier orbitals reported in Table 4 for complexes of D_{3d} symmetry and in Table 5 for complexes of C_{2h} symmetry correspond to the $1\pi-3\pi$ and $1\delta-2\delta$ orbitals whose progressive occupation by the fragments d electrons determines the VB description of the M−C and C−C bonds. This group of orbitals is by far the most important and will be discussed in more detail by studying the influence of the fragment d configuration, the nature of the metal, and its oxidation state in the $[\{(OH)_3M\}_2(\mu\text{-}C_2)]$ (M = Ti, V, Cr, Mn) and the $[\{(H_2O)_n(OH)_{3-n}Cr\}_2(\mu\text{-}C_2)]$ (n = 0, 1, 2) series. Figure 4 shows the progressive filling of the frontier orbitals in the $[\{(OH)_3M\}_2(\mu\text{-}C_2)]$ (M = Ti, V, Cr, Mn) series and illustrates the effect of the electron count on orbital energies. For this series, the main frontier orbitals are $6e_u$, $6e_g$, $7e_u$, and $7e_g$, as described in Table 4. From the discussion above, we see that they correspond to the 1π, 2π, 3π and 1δ, 2δ orbitals, respectively. The 1π orbital, which has an almost pure π (C_2) character, is fully occupied in all the considered complexes. It is the HOMO in the $[\{(OH)_3Ti\}_2(\mu\text{-}C_2)]$ complex, made up by $Ti(OH)_3$ (d^1) fragments, which has therefore a formal acetylenic M−C≡C−M structure. The next orbital to be occupied in the $[\{(OH)_3V\}_2(\mu\text{-}C_2)]$ and $[\{(OH)_3Cr\}_2(\mu\text{-}C_2)]$ complexes, made up of $V(OH)_3$ (d^2) and $Cr(OH)_3$ (d^3) fragments, is the $6e_g$ (2π) which has a relevant π^* (C_2) character and leads to formal M═C═C═M and M≡C−C≡M VB structures. The next to be filled in the $[\{(OH)_3Mn\}_2(\mu\text{-}C_2)]$ complex, made up by $Mn(OH)_3$ (d^4) fragments, is the $7e_u$ (3π) with partial π (C_2) character which leads to a M═C═C═M structure. These results are in perfect agreement with the qualitative conclusions above. In addition, a careful analysis of these frontier orbitals and of their changes with the fragment d configuration enables one to discuss in more detail various geometrical and electronic aspects. It is found that passing from Ti to Mn there is a progressive increase in the metal contribution to the $6e_u$ and $7e_u$ orbitals, of $d_\pi-\pi$ character, and a decrease in the metal contribution to the $6e_g$ orbital, of $d_\pi-\pi^*$ character. This can be easily explained by noting that the d-orbital energies of the $M(OH)_3$ fragments decrease going from the left to the right in the transition series, as illustrated in the orbital diagrams reported in Figure 2. This effect reflects the increase in electronegativity along the transition series. For example, it explains why the Mn complex, which has the same formal cumulenic structure of the V complex, has a longer C−C and a shorter M−C bond length. This effect can be also pointed out by a Mulliken population analysis. According to such analysis, the population acquired by the C_2 orbitals of σ symmetry decreases from Ti to Mn and, at the same time, there is a decrease in the overall charge on the metal atom. These effects show an increase of the $C_2 \rightarrow M$ σ donation and are both a direct consequence of the mentioned increasing electronegativity along the transition series. On the other hand, the population of the C_2 π orbital decreases and that of the C_2 π^* orbital increases from Ti to Cr, showing an increase of both the $C_2 \rightarrow M$ π-donation and the $M \rightarrow C_2$ π^*-back-donation. This behavior reflects both the progressive population

of the $6e_g$ orbital with relevant π^* (C_2) character and the decrease of the metal d_π energies.

An analogous situation, although with a slightly different frontier orbitals ordering, is found when we consider the $[\{(H_2O)_n(OH)_{3-n}Cr\}_2(\mu\text{-}C_2)]$ (n = 0, 1, 2) series. Figure 5 shows the progressive filling of the frontier orbitals in this series, illustrating the effect of the electron count on orbital energies. The situation is now complicated by the lower symmetry, C_{2h}, which removes the degeneracy of the *e* orbitals and mixes the d_σ, d_π, and d_δ components. For this series, the main frontier orbitals are $7a_u$, $12b_u$, $7b_g$, $13a_g$, $8a_u$, $14b_u$, $13b_u$, and $14a_g$, as reported in Table 5. The first three pairs of orbitals above correlate with the $6e_u$, $6e_g$, and $7e_u$ orbitals of the D_{3d} group and correspond with the 1π, 2π, and 3π orbitals, respectively, while the remaining pair corresponds to 1δ and 2δ orbitals. In the $[\{(OH)_3Cr\}_2(\mu\text{-}C_2)]$ complex, made up of $Cr(OH)_3$ (d^3) fragments, the $6e_g$ (2π) is fully occupied leading to a formal M≡C−C≡M VB structure. The next two orbitals to be filled in the $[\{(H_2O)(OH)_2Cr\}_2(\mu\text{-}C_2)]$ and $[\{(H_2O)_2(OH)Cr\}_2(\mu\text{-}C_2)]$ complexes, made up of $Cr(OH)_2(H_2O)$ (d^4) and $Cr(OH)(H_2O)_2$ (d^5) fragments, are the $13b_u$ and $14a_g$ (of δ character) so that the corresponding complexes maintain a M≡C−C≡M structure. These results differ from those obtained for the $[\{(OH)_3M\}_2(\mu\text{-}C_2)]$ (M = Ti, V, Cr, Mn) series in which the 3π orbitals were occupied before the 1δ and 2δ ones. This behavior can be ascribed to the stabilization of the fragment d_δ orbitals due to a strong mixing with the d_σ components and due to the reduced interaction with the ligands, one or two H_2O molecules replacing OH^- ligands. Again, a careful analysis of the frontier orbitals and of their changes with the fragment d configuration permits a more detailed discussion of the geometrical and electronic aspects. We found that, passing from Cr(III) to Cr(I), there is a progressively slight decrease of the metal contribution to the $7a_u$ and $12b_u$ orbitals (of d_π−π character) and a relevant increase of the π^* (C_2) contribution to the $13a_g$ and $7b_g$ orbitals (of d_π−π^* character). This can be easily explained as before, noting that the d-orbital energies of the $Cr(OH)_{3-n}(H_2O)_n$ fragments increase in going from Cr(III) to Cr(I), as illustrated in the orbital diagrams reported in Figure 3. This explains the slight elongation of the C−C bond length along the series in spite of the same formal M≡C−C≡M structure.

Energy Decomposition and Bond Analysis. In the discussion of the bonding in these complexes, it is useful to point out the relative magnitudes of the main interactions and the strengths of the bond between the two metal fragments and the central C_2 unit. The total energy for the dissociation of the $[\{(H_2O)_n(OH)_{3-n}M\}_2(\mu\text{-}C_2)]$ complex into a C_2 and two $[M(H_2O)_n(OH)_{3-n}]$ fragments can be broken down as follows:

$$\Delta E = \Delta E^0 + \Delta E^{prep} + \Delta E^{el} \quad (1)$$

where ΔE^0 is the steric repulsion between the C_2 molecule and the two $[M(H_2O)_n(OH)_{3-n}]$ fragments, ΔE^{el} is the electronic interaction energy, and ΔE^{prep} accounts for the energy required to distort C_2 and the two fragments from their ground state geometries to the geometries they adopt in the final complexes, in the proper valence states.[26]

Table 6. Decomposition of the Total Bond Energy (eV) into Contributions from Different Symmetries for the Decomposition of Titanium, Vanadium, Chromium, and Manganese Complexes (D_{3d} Symmetry) into C_2 and the Corresponding Metal Fragments

param	$Ti_2C_2(OH)_6$	$V_2C_2(OH)_6$	$Cr_2C_2(OH)_6$	$Mn_2C_2(OH)_6$
$\Delta E_{a_{1g}}$	−109.7	−87.1	−77.8	−45.5
$\Delta E_{a_{2u}}$	−137.7	−106.2	−93.7	−63.3
ΔE_{e_g}	−2.8	−210.8	−406.1	−270.1
ΔE_{e_u}	−9.5	−14.5	+69.3	+7.6
$\Delta E^0+\Delta E^{el}$	−225.1	−235.2	−255.9	−178.9

A better insight into the electronic factors governing the relative stability of the $[\{(H_2O)_n(OH)_{3-n}M\}_2(\mu\text{-}C_2)]$ complexes is provided by the analysis of the electronic interaction energy in terms of the different symmetries:

$$\Delta E^{el} = \sum_\Gamma \Delta E_\Gamma \quad (2)$$

This is particularly useful for the D_{3d} complexes, see Table 6, for which $\Delta E_{a_{1g}}$ and $\Delta E_{a_{2u}}$ represent the contributions to ΔE due to the metal−carbon σ interactions, ΔE_{e_g} represents the contribution due to the back-donation from the metal to the antibonding π^* orbitals of C_2, and ΔE_{e_u} represents the contribution due to the donation from the C_2 π orbital to the empty metal orbitals. The contributions from other symmetries are negligible. One of the main contributions to the stability of all the considered complexes is that from the a_{1g} and a_{2u} symmetries, associated with the metal−carbon σ bonding, which varies slightly among the various complexes with a steady decrease in going from the left to the right of the transition series and a more relevant decrease for manganese. The contribution from the e_g symmetry, associated with the back-donation from the metal d_π orbitals to the π^* orbitals of the C_2 moiety, strongly depends on the occupation of the 2π orbital. Therefore, it is negligible for titanium, where the 2π level is empty, and relevant (similar to that from σ bonding) for vanadium, where 2π is doubly occupied, and has an almost double value for chromium, where 2π is quadruply occupied. The contribution is smaller for manganese, although 2π is still doubly occupied, because of the reduced M → C_2 donation due to the higher metal electronegativity. The contribution from e_u is small and even positive; it gives less direct information since it is determined by a compromise between the stabilizing bonding metal−carbon π interactions in the 1π orbital and the destabilizing antibonding metal−carbon π interactions in the 3π orbital.

In Table 6, we also report $\Delta E^0 + \Delta E^{el}$, which is an overestimated evaluation of the binding energy between C_2 and the two metal fragments which neglects the preparation energy. Although the preparation energy may vary in a relevant way among different complexes, its value is in the range 60−100 kcal mol^{-1} (*e.g.* 67 kcal mol^{-1} for the vanadium complex) so that the corrected binding energies remain fairly high. We also see that the titanium, vanadium, and chromium complexes have similar values of about 225−255 kcal mol^{-1}, while the

(26) Ziegler, T. *A General Energy Decomposition Scheme for the Study of Metal-Ligand Interactions in Complexes, Clusters and Solids*; NATO ASI C378; Kluwer: Boston, MA, 1992.

manganese complex has a lower value of 179 kcal mol^{-1}. The bonding energy is expected to be even lower going to the right of the transition series due to an increase in the metal electronegativity and the further population of the 3π level. This could explain why μ-C_2-bridged complexes of class I are observed only for early transition metals.

Magnetism. For the $[\{(OH)_3V\}_2(\mu\text{-}C_2)]$ complex of D_{3d} symmetry, with a d^2 configuration for the $V(OH)_3$ fragment, the 2π orbital is occupied by two electrons, and the double degeneracy of this level let us forecast a triplet ground state. Two of the three experimentally synthesized complexes for which the fragments have this configuration, *i.e.* the tantalum and titanium complexes $[\{^tBu_3SiO)_3Ta\}_2(\mu\text{-}C_2)]$ (**1**)[4] and $[\{Et_8N_4)_3Ti\}_2(\mu\text{-}C_2)Li_2]^{2-}$ (Et_8N_4 = *meso*-octaethylporphyrinogen) (**2**),[6] show an anomalous magnetic behavior while the remaining one, $[\{Cp_2(PMe_3)Ti\}_2(\mu\text{-}C_2)]$ (**3**),[7] is diamagnetic. In particular, the magnetic susceptibility of $[\{^tBu_3SiO)_3Ta\}_2(\mu\text{-}C_2)]$ has been accurately studied[4] and shows a peculiar temperature dependence which has been explained in terms of a large temperature-independent paramagnetism (TIP).

The presence of a large TIP is due to the mixing of thermally inaccessible paramagnetic excited states with the singlet ground state via second-order Zeeman terms in the perturbative expression of the electronic energy in the precence of a magnetic field. Although such a large TIP term would require the availability of low-lying paramagnetic excited states, their thermal inaccessibility impose a minimum gap of the order of 1000 cm^{-1}.

Concerning the two titanium complexes, **3** is diamagnetic and therefore has a well-isolated singlet ground state,[7] while **2** is paramagnetic, although the available magnetic data do not allow a clear attribution of a triplet ground state.[6]

Among the three possible states arising from the $(e_g)^2$ configuration, our calculations have led to a triplet $^3A_{2g}$ ground state for the $[\{(OH)_3V\}_2(\mu\text{-}C_2)]$ complex, with the lowest $^1A_{1g}$ singlet state 0.43 eV above and a second ^1E_g singlet state 0.68 eV higher. A similar behavior had been found in extended Huckel calculations on the $[\{^tBu_3SiO)_3Ta\}_2(\mu\text{-}C_2)]$ complex[4] and the disagreement with the experimental data was explained by a suggestion that the distortion of the MCCM bridge from linearity (the observed ∠TaCC angle is 173°) would stabilize the orbitally degenerate ^1E_g singlet state through a first-order Jahn−Teller effect which relieves its degeneracy. Indeed, all other synthesized complexes with a d^2 fragment configuration have a MCCM bridge significantly distorted from linearity with a ∠MCC angle close to 170° and a *trans* conformation. To better check this interpretation, we calculated the triplet−singlet separation for $[\{(OH)_3V\}_2(\mu\text{-}C_2)]$ as a function of the ∠VCC angle.

For ∠VCC angles lower than 180°, the molecule belongs to the C_{2h} point group and the $^3A_{2g}$, $^1A_{1g}$, and ^1E_g states of the D_{3d} complex correlate with the ^3B_g, ^1A_g, and $^1A_g + {}^1B_g$ states, respectively. On lowering the ∠VCC angle, we expect that, among the three possible singlet states, the lowest ^1A_g does not vary too much in energy while the ^1A_g state correlating with ^1E_g is stabilized and the remaining ^1B_g state is destabilized. Indeed, the results obtained for the three triplet−singlet separations at a few angles lower than 180° confirm these previsions and only the $^3B_g-{}^1A_g(^1E_g)$ triplet−singlet separation decreases, although very slowly, so that the triplet remains the ground state even at 150° with the lowest stabilized $^1A_g(^1E_g)$ still 0.55 eV above. Therefore, for the considered $[\{(OH)_3V\}_2(\mu\text{-}C_2)]$ complex, the ground state is a triplet irrespective of the distortion from linearity. This result is compatible with the magnetic data observed for complex **2** but does not match with the data for compounds **1** and **3**. However, this latter disagreement is not surprising in view of the different metal and ligands employed in the model calculation. Moreover, such a result confirms the importance of the triplet state in the few synthesized complexes with a d^2 fragment configuration and supports the interpretation of the magnetic behavior of **1** in terms of a large temperature-independent paramagnetism.

It is worth noting that the low energy of the triplet state is not to be interpreted on the basis of an antiferromagnetic interaction between the two metal centers through the C_2 bridge. Indeed, the availability of this low-lying triplet cannot be attributed to a small interaction between the magnetic orbitals on the two metal fragments (essentially d_π) but, rather, to the high symmetry of this molecule which allows the presence of a half-occupied, doubly-degenerate LUMO level. Actually, the magnetic orbitals of the metal fragments strongly interact with the π orbitals of the C_2 bridge forming a low-energy MO which describes a fairly strong metal−carbon bond. Therefore, the magnetic behavior of these dinuclear complexes bears no direct resemblance to the magnetic properties of the constituting metal fragments.

Concluding Remarks

The main purpose of the present investigation has been to reveal the factors governing the interaction mode of a bridging μ-C_2 unit in dinuclear complexes. Our calculations allowed us to identify two classes of dicarbido compounds, depending on the metal, its oxidation state, and the nature of the ligands. Early transition metals of the titanium, vanadium, and chromium triads, in high oxidation states with mainly π-donor ligands like RO^- in a pseudotetrahedral coordination, constitute one of the classes. Within this class, the d^n configuration is the prominent factor determining the interaction mode, namely M−C≡C−M, M=C=C=M, or M≡C−C≡ M. In the second class, we found late transition metals from the manganese triad to the right, in low oxidation states with mainly π-acceptor ligands like carbonyl or pentadienyl, in a pseudo-octahedral coordination. For this latter class, only the acetylenic μ-C≡C structure has been found, irrespective of the metal d configuration.

The results of the density functional calculations on complexes of the first class have been generalized to a simple molecular orbital model which allows the prediction of the limiting bonding mode of the C_2 unit in these dinuclear complexes. The parameters which have been used to predict the interaction mode of the C_2 unit are the oxidation state and the d^n configuration of the metal in the neutral metallic fragment, regardless of the values conventionally determined for the same metal parameters in the overall complex.

Chart 4

Fragment *d* configuration	Bond character
d^1	$M - C \equiv C - M$
d^2	$M = C = C = M$
d^3	$M \equiv C - C \equiv M$

As long as π-donor ligands are considered, so that the metal d orbitals are not too low in energy, the VB structure of μ-C_2-bridged dinuclear complexes of early transition metals depends on the electron count up to d^3 as shown in Chart 4.

These predictions have a very strong support in experimental results for the early metal transition area, while complexes where the metal fragment has a d^4 or d^5 configuration have not yet been reported. This notwithstanding, we can foresee for a d^4 configuration either a M≡C—C≡M or a M═C═C═M structure, depending on the energies of the d_π orbitals. Low-energy d_π orbitals, like in Mn(III), will favor the acetylenic structure, while higher energy d_π orbitals, as in Cr(II), will favor the cumulenic one. The same factors will discriminate between the M≡C—C≡M and the M—C≡C—M interaction modes for a d^5 configuration.

The M═C═C═M and M≡C—C≡M bonding interactions of the C_2 unit require d_π empty orbitals which are available in poor d^n electron configurations of early transition metals. The π-donation of the C_2 unit to the metal is prevented in late transition metals in a low oxidation state; thus, the only interaction mode occurring here is the diacetylenic form, M—C≡C—M, as predicted by the theory and found experimentally.

Acknowledgment. The present work has been carried out within the COST D3 Action. We thank the CINECA for providing a computer grant. Support by the Fond Nationale Suisse de la Recherche Scientifique and the Italian CNR is gratefully acknowledged.

OM9603676